Construction and Building Materials 219 (2019) 154–163

Contents lists available at ScienceDirect

Construction and Building Materials

journal homepage: www.elsevier.com/locate/conbuildmat

Stone consolidation with SiO_2 nanoparticles: Effects on a high porosity limestone

Emilia Vasanelli [a], Angela Calia [a,*], Maurizio Masieri [a], Giovanni Baldi [b]

[a] CNR-IBAM, National Research Council – Institute for Archaeological Heritage, University Campus, Prov.le Lecce Monteroni, 73100 Lecce, Italy
[b] Ce.Ri.Col – Colorobbia Research Centre, Via Pietramarina, 53 50053, SOVIGLIANA, Vinci, FI, Italy

HIGHLIGHTS

- Performances of a SiO_2 NPs based consolidant were investigated on a porous limestone.
- The nanosilica treatment was compatible with the physical properties of the stone.
- Surface hardness and UPV tests detected increased stone cohesion.
- Irregular penetration depth led to heterogeneous nanoSiO_2 distribution into the stone.
- Porosimetric changes due to nanofillers increased salt damage for consolidated stone.

ARTICLE INFO

Article history:
Received 31 December 2018
Received in revised form 2 April 2019
Accepted 27 May 2019
Available online 4 June 2019

Keywords:
Stone consolidation
Nanosilica
Porous limestone
Penetration depth
Surface hardness
UPV
Physical characterisation
Durability

ABSTRACT

This study deals with the effect of a water colloidal suspension of nanosilica applied as a consolidant on a porous limestone. The stone performances were investigated by several analyses and tests. They fulfilled basic requirements such as consolidating effectiveness and compatibility with the original colour and water transport properties. A point of weakness was found in the behaviour under the salt crystallisation test, showing a decreased durability for the treated stone. The modification of the porous structure accounts for this result, suggesting that the distribution of the nanoparticle fillers into the stone substrate should be improved.

1. Introduction

Conservation and enhancement of the Cultural Heritage not only come from the need of preserving the identity values of the social communities, but a renewed interest toward these activities by the modern societies also moves from economic reasons, as Cultural Heritage may represent one of the most important income of the tourism industry in many countries.

Preservation activities to large extents involve stone buildings and monuments, as an important part of the Cultural Heritage, which is exposed to a high damage risk in outdoor conditions. Natural stones under the complex of environmental factors undergo a variety of deterioration processes promoted by chemical, physical and biological agents [1]. The incidence of the weathering in the exposure contexts is strictly related to the stone's inherent factors, including mineralogical-chemical composition and petrophysical features. Very often a dramatic deterioration affects stone cohesion to a certain depth, leading to material loss from the surface. In such material conditions, consolidation may be effective to achieve a partial recovery of the physical–mechanical properties of the deteriorated stone through binding disintegrated grains with products penetrating into the pores.

At this purpose, mostly organic-based products are used. Alkoxysilanes, and in particular tetraethoxysilane (TEOS) and methyltrimethoxysilane (MTMOS), have been dominant in the conservation practice, mainly due to their ability to penetrate easily into porous materials and the lesser impact on the permeability and drying properties of the consolidated stones, compared

* Corresponding author.
E-mail addresses: e.vasanelli@ibam.cnr.it (E. Vasanelli), a.calia@ibam.cnr.it (A. Calia), baldig@colorobbia.it (G. Baldi).

https://doi.org/10.1016/j.conbuildmat.2019.05.169
0950-0618/

to other organic-based products [2]. The main issues with such products consist of cracking during the drying due to gel shrinkage, temporary hydrophobic behaviour, influence of the environmental conditions on the gel polymerization [3,4] and a poor chemical affinity between calcite and the silica molecules formed after their hydrolysis and condensation [5]. Acrylic-based resins [6] and epoxy resins [7] have been also used and their drawbacks, such as changes of physicochemical properties of the stones and detrimental effects due to long-term ageing, are well known [8,9].

Inorganic consolidating products, such as calcium hydroxide, barium hydroxide and ammonium oxalate have a good durability and a high compatibility with the stone components [10], but they exhibit a lower penetration ability and a subsequent poor strengthening effect compared to organic products. Encouraging results have been obtained in recent years for phosphate-based treatments in alternative to inorganic traditional materials [11,12].

Consolidation treatments encompass a wide range of issues [13]. A high level of risk is related to their application, as the introduction of the products into the porous network may strongly change the stone characteristics and properties, thus causing unwanted effects or further damage. Moreover, such treatments are substantially irreversible, because the consolidating products hardly can be removed, once they penetrate into the stone structure. Therefore, they must ensure at least the retreatability of the substrates. Stone consolidation deserves a great attention and the research of effective consolidating treatments for the different stone types and deterioration processes is a great challenge for the conservation science [14]. New systems have been explored in recent years, through the application of the nanomaterial science in the stone conservation field. An approach consisted of the development of hybrid (organic-inorganic) nanocomposites, addressing the improvement of the gel phase physical properties and consequent performances of alkoxysilane based consolidants, through the modification of such products with the use of nanoparticles, such as colloidal oxides, nano-calcium oxalate, etc. [15,16].

In the field of the inorganic consolidation products, colloidal dispersion of nanoparticles have been designed on the basis of new synthesis routes, with promising advantages in terms of penetration depth due to the small size of the nanoparticles, an increase in the surface available to react and a high speed of reaction [17,18]. They include inorganic nanoparticles of calcium, magnesium, strontium hydroxides, etc., as well as of silica, which is the most used strengthening agent. Some studies investigated the performances of colloidal dispersions in water of SiO_2 NPs on some stone substrates [19,20] and in comparison with traditional inorganic consolidants [21]. Some issues with different application methods [22] and distribution of the product within the stone [23] have been evidenced. Drawbacks due to accumulation of silica NPs within the stone [24] and the influence of RH on the consolidating effectiveness [25] and durability performances, as well, [26] have been reported. A more comprehensive knowledge of the performances of such consolidating products on the different stones is suitable, as interactions between the nanoparticle dispersions and porous substrates may be different as a function of the characteristics of both stones and products. In this paper the effects of a colloidal dispersion of nanosized SiO_2, have been investigated on a porous limestone. The study moves from a collaboration activity with the Cericol Research Center of the Colorobbia (Italy), which formulated the product, already used for the consolidation of the marble capitals of the Pisa Tower [27,28].

The effectiveness of the consolidation treatment was evaluated by measuring the distribution and penetration depth of the silica nanoparticles into the stone by Environmental Scanning Electron Microscopy coupled with Energy Dispersive Spectrometry (ESEM-EDS). The hardening effect on the treated stone surface was measured by abrasion and penetrometric tests. The compatibility of the treatment with the substrate characteristics and properties was assessed by measuring changes of surface colour, microstructural features and behaviour against the water. The performances of the treatment as regard the durability of the treated stone was investigated under a salt crystallization test. Finally, measurements of ultrasonic pulse velocity (UPV) were performed to detect the presence of the product within the stone and the increased stone cohesion, as well as the salt damage, which was also evaluated through weight loss measurements.

2. Materials and methods

2.1. Materials and treatment application

The product used for the stone consolidation consists of nanosized SiO_2 dispersed in water (30% w/w). It has a density of 1.2 g/mL, a viscosity of 12 mPas/sec at 20 °C and a pH of 10.5. The synthesis procedure is based on the hydrolysis in water of the tetraethyl orthosilicate $Si(OC_2H_5)_4$, through the following reaction:

$$Si(OR)_4 + H_2O \rightarrow HO - Si(OR)_3 + R - OH$$

Water and catalyst to suitable amounts allow to obtain a complete replacement of the OR groups by the OH groups. In addition, a condensation reaction takes part to form a siloxane [Si-O-Si] bond from the partially hydrolysed molecules. Then, the sol is destabilized arranging a pH value < 4.0. The residue is washed, dried at 80 °C and re-dispersed in water to a pH value > 9.0. A stable nanodispersion of rounded silica particles is obtained, with NPs having a mean size of approximately 30 nm (PdI 0.40) and a Z-potential of 35 mV.

A soft, very fine and whitish limestone, with an integral open porosity of 30%, approximately, was used for the application of the treatment. The stone, locally named "Pietra Gentile" or "Carovigno stone"[29], has been widely found in the historic-architectural heritage of the Puglia region (Southern Italy). Petrographically, it is a medium-fine wackestone [30], made of fine bioclastic remains and lythoclasts (Fig. 1), with sizes from some tens of microns up to 200 μm, within a micritic groundmass. This is finely mixed with small amounts of microcrystalline calcitic cement. A fine porosity of both interparticle and vug types is widespread throughout the groundmass.

Samples of different sizes were used for the application of the treatments, depending on the different tests and analyses to be performed. After the cutting and cleaning with a soft brush, they were washed with deionized water in order to remove the stone dust and then dried in oven at 60 °C. The dry weight was assumed when the difference between two consecutive weight measurements was less than 0.1% of the initial weight. Before the treatments, the samples were stabilized at the laboratory controlled conditions (22 ± 2 °C, 45 ± 5% R.H.) for 24 h. Such conditions persisted during the treatment and during a curing period of one month.

On the basis of previous findings [22], the optimal procedure for the treatment consisted of consecutive applications by brush of 100 mg/cm^2 of the solution, which corresponds to an amount of silica nanoparticles of 30 mg/cm^2.

The weight increase was measured on the samples immediately after the application of the product and after one month of curing. An analytical balance (Model BP 2215, Sartorius AG) with an accuracy of ±0.1 mg, was used.

The weight increase is reported in Table 1 for five cubic specimens having 5 cm side, which were treated on the overall surface. Just after the treatment the product applied was approximately 6% of the dry weight. After one month, the final residue left within the stone pores was 1.42%.

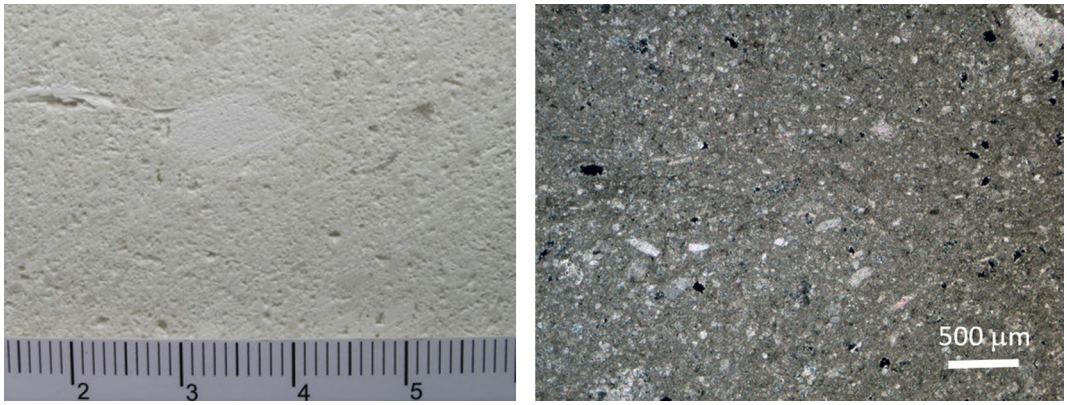

Fig. 1. Macroscopic appearance of the Carovigno stone (left) and thin section image under crossed nicols (right), showing fine fossil remains within a micritic groundmass with a poor microsparitic cement.

Table 1
Applied product amounts (mg/cm^2) measured just after the application of the treatment and after one month of curing.

Sample	5 × 5 × 5 cm sample size		Sample	10 × 10 × 2 cm sample size	
	Product amount just after the application (mg/cm^2)	Product amount after curing (mg/cm^2)		Product amount just after the application (mg/cm^2)	Product amount after curing (mg/cm^2)
S1	98.87	24.60			
S2	99.80	21.73			
S3	99.47	23.93			
S4	99.13	25.13	S1a	99.98	26.85
S5	100.00	22.67	S2a	99.25	25.25
Mean ± St. Dev.	99.45 ± 0.47	23.61 ± 1.40		99.62 ± 0.52	26.05 ± 1.13

3. Analyses and tests

Several analyses and tests were performed on the untreated samples and on the treated ones, after one month from the treatment.

The distribution of the treatment on the stone surface and the penetration depth of the nanosilica particles within the stone were evaluated as follows.

- Morphological observations of the treated and untreated surface were performed by Environmental Scanning Electron Microscopy (Mod. XL30, FEI Company) Energy-Dispersive X-ray Spectroscopy combined with the ESEM was used on sample cross sections for qualitative/quantitative elemental analyses of Si as an indicator of the product into the stone. The following analytical conditions were adopted: low vacuum mode, pressure of 0.7 Torr, beam accelerating voltage of 25 kV, 100 Lsec acquisition time, 100 × 100 µm area of each analysis. The obtained EDS spectra were normalized to the Ca peaks.
- Ultrasonic Pulse Velocity measurement, as a non-destructive test, was performed on the stone samples before and after the treatment to verify changes in the velocity propagation due to the application of the treatment. UPVs were measured according to the standard [31] by a direct transmission method. An Epoch 4 plus (Olympus) instrument and probes with a frequency of 1 MHz were used. A good contact between the transducers and the stone was ensured by a coupling gel. UPV measurements were repeated three times in each measuring point and the mean value was calculated. The test was performed on ten cubic specimens of 5 cm side, including five untreated samples and five samples treated with nanosilica on their overall surface. Three points of measurement along each direction (x, y, z) were considered and velocities were expressed as the mean of the obtained values. Two specimens measuring 10 × 10 × 2 cm were also used. In that case, before and after the treatment that was applied on the largest 10x10 cm faces, velocities were measured across the thickness of 2 cm, at four different points.

The surface hardness increase on the treated stone was assessed by the following mechanical tests.

- Abrasion test according to the standard [32]. This destructive test determines the abrasion resistance of the stones, by measuring the length of a groove produced by a disc with a thickness of 70 mm that rotates on the specimen surface at a controlled speed and a constant pressure. Three specimens 10 × 10 × 7 cm were used for the test. They were tested on the two largest faces, namely 10 × 10 cm, one of which was treated with nanosilica. Penetration test, as a moderately destructive test, was also performed. An RSM (Response Surface Methodology) penetrometer (RSM_15 by DRC srl) was used. This instrument was designed to estimate the resistance of mortar joints to the penetration of a steel needle driven by strikes generated at a constant energy of 4.55 Nm. The result of the test is a curve of the penetration depths (expressed in millimetres) versus the number of the applied strikes. The penetration depth can be used as a parameter to evaluate the surface hardness of different samples in a comparative way: at each number of strikes, the higher the value of the penetration depth the lower the hardness of the surface. A stone ashlar of 38 × 31 × 12 cm size was used for the test. This was performed on the two largest faces of 38x31 cm size, one of which was treated with the nanosilica based product. Five measuring points were considered for each treated and untreated face and the mean value was calculated at a fixed number of strikes.

The compatibility of the treatment with the original stone colour properties, microstructure features and behaviour against water was verified by the following analyses and tests.

- Colour changes due to the application of the treatment were evaluated by a colorimetric analysis [33], using a reflectance colorimeter (Chroma Meter Minolta CR 300) with a CIE standard illuminant C. The colour parameters L * a * b *were determined in the CIELab 1976 colour space. Ten measurements were taken on each sample area measuring 5 × 5 cm. The colour variations (ΔE*) were calculated as:

$$\Delta E* = [(\Delta L*)^2 + (\Delta a*)^2 + (\Delta b*)^2]^{1/2} \quad (1)$$

where L* is the lightness/darkness coordinate, a* and b* the red/-green and yellow/blue coordinates, respectively.

- Porosity and porosimetric analyses by Mercury Intrusion Porosimetry in the range of 0.001–100 μm, using Pascal 140 Series and Pascal 240 Series mercury-intrusion porosimeters (Thermo Finningan) were performed on three samples of each untreated and treated stone. The latter was investigated over a sample thickness of 5 mm from the treated surface.
- Static contact angle measurements [34] were performed by means of a Costech apparatus. Ten measurements were performed on each sample area of 5 × 5 cm.
- Water vapour permeability [35] was measured on 5 specimens measuring 5 × 5 × 1 cm, treated on one of the two largest faces, namely 5 × 5 cm; the results were expressed as the mean value. The water vapour permeability is defined as the mass of water vapour transmitted through a sample per area unit in a time unit, under defined conditions, and describes the ability of a material to allow water vapour passing through. The following equation was used to calculate the water vapour permeability:

$$WVP = \frac{\Delta M}{(t * A)} \quad (2)$$

where ΔM is the weight change in the steady state (expressed in g), A is the exposed area to water vapour (in m^2) and t is the unit time (24 h). In all the cases, the used ΔM was the average of three consequent values of the daily difference in weight.

- A capillarity water absorption test [36] was performed on 5 specimens measuring 5 × 5 × 2 cm, treated on one of the two largest face, namely 5 × 5 cm. Progressive weight increases of the samples were measured and the amount of absorbed water (Q) was calculated as follows:

$$\boldsymbol{Q_i} = \frac{(\boldsymbol{w_i} - \boldsymbol{w_0})}{\boldsymbol{S}} \quad (3)$$

where: w_i and w_0 are the weight of the sample at time t_i and t_0, respectively, and S is the area of the sample exposed to the water.

Finally, the resistance to the salt crystallization of the treated stone was evaluated in comparison to the untreated one, by performing an accelerated aging test according to the standard [37]. Ten cubic specimens, 5 cm side, were tested, including five untreated samples and five samples treated on the overall faces. Fifteen ageing cycles were carried out. After each one, the specimens were visually inspected and their weight loss was registered. Damage was also checked by UPV measurements performed on the cubic specimens before the salt crystallisation test and at the end of each test cycle, following the above mentioned procedure of measurement.

4. Results and discussion

4.1. Effectiveness

4.1.1. Distribution and penetration depth

Effectiveness, compatibility and durability with respect to the original characteristics and properties of the stone are the main requirements to be assessed in evaluating the performances of a conservation treatment. In the case of a consolidating treatment, the effectiveness comes from the ability of the consolidant to penetrate homogeneously and deep enough into the substrate and to increase the mechanical performance of the treated surfaces.

The method of the application and the amount of the product to be applied are discriminating parameters with respect to the superficial distribution and penetration of the treatment and they should be tuned to the specific stone characteristics [38]. Observations by ESEM showed a grain shaped morphology of the treated stone surface (Fig. 2). Nanosilica was in the form of agglomerations and accumulation in the form of cracked layers, often found on the stone surface [21,24] was not observed. This result comes from the optimal applied product amount and treatment procedure. These were selected on the basis of a previous screening [22], showing that accumulation of the product and micro-crack formation took place when exceeding amounts were used, without any improvement of the penetration.

Being the Carovigno stone a pure limestone, almost exclusively made of calcite [29], Si is an effective marker for the evaluation of the amounts of the product at different depths within the treated stone. The profile of Si amounts in Fig. 3, as measured by the EDS analysis up to a depth of 8 mm, shows the highest concentration on the surface (9.57% wt). At 0.5 mm of depth it was 40% less than the amount measured on the surface, then a progressive reduction of the Si content was detected, up to match that found in the untreated stone.

According to the literature [20], ultrasonic pulse velocity test was able to detect the presence of the nanosilica based treatment through higher velocities of propagation recorded in the treated stone samples. Such an increase was found in all the measuring points of the samples across the thickness of 2 cm (Fig. 4a) and it was 4.5%, on average, which is comparable to the entity recorded by Zornoza-Indart & Lopez-Arce [25] after the consolidation of a bioclastic calcarenite. The test performed on the samples of 5 cm side yielded different results. In the untreated stone specimens UPVs varied between 3400 m/s and 3900 m/s. After the treatment they remained almost unchanged (Fig. 4b), with a maximum variation of not more than 2%. The difference in the UPV results obtained for slab and cube samples may be due to the fact that the contribution given by the consolidated stone layers - which are limited to a few millimetres - to the wave propagation along the overall path within the cubic specimens, was negligible compared to the preponderant one arising from the thick untreated stone portions investigated across the samples, which accounts for the almost unchanged velocity values. The relative incidence of the treated stone layers on the wave propagation was higher across the thin slabs, being the wave path within the untreated stone in these samples shorter compared to the thick cubes, and in this case it was appreciable as a velocity increase. In fact, the ultrasonic velocity propagation within the stone materials depends on a variety of factors relating to both composition and physical-mechanical characteristics [39–41]. These characteristics may be modified by the application of a consolidating product and the consequent wave velocity variations may be used as an index of the presence and/or the effectiveness of the consolidation treatment [11,25,42]. In the light of the results of the surface hardness measurements reported in the next paragraph, the velocity increases – although detected to different extents depending on the thick-

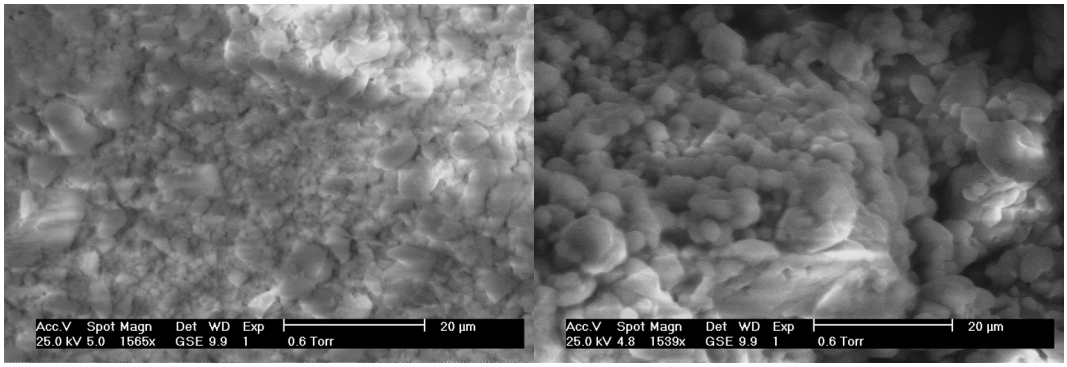

Fig. 2. ESEM micrographs of the surface of untreated (left) and treated (right) samples, showing nanosilica on the treated surface in the form of agglomerations with grain shaped morphology, while no accumulation as xerogel cracked layers is evident.

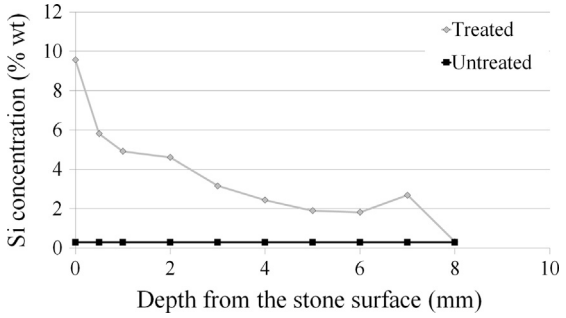

Fig. 3. Profile amounts of Si detected by EDS analysis on cross sections of treated and untreated samples.

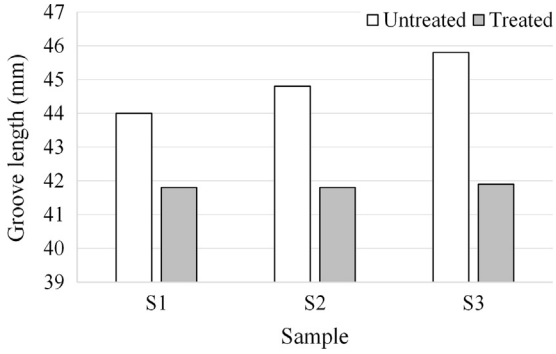

Fig. 5. Groove lengths as measured by the abrasion test on treated and untreated surfaces of each specimen.

nesses of the investigated samples - may be not only attributed to the changes of the stone composition and microstructure due to the introduction of the silica nanofiller into the pore network, but they testify the effectiveness of the consolidation treatment in increasing the stone cohesion, according to [25].

4.1.2. Surface hardness

The results of the wide wheel abrasion test showed an improvement of the surface hardness for the consolidated samples. The length of the grooves due to the abrasion wheel was about 7%, on average, lower than those measured on the untreated samples (Fig. 5).

This test has a high destructive impact and, in addition, it may be performed only in laboratory conditions. On the contrary, mechanical penetration tests have a low destructiveness and they may be performed on real site conditions. Therefore, in comparison to the previous abrasion test, a penetrometric test was also performed and results obtained at 1, 5, 10 and 15 strikes driving the steel needle into the stone, are reported in Fig. 6. They show different responses from treated and untreated samples up to 10 strikes, with a lower penetration of the needle in the former. Up to 10 strikes the test investigated about 8 mm from the surface in the treated stone and showed a consolidating effect likely relating to the presence of nanosilica particles up to this depth, although this was more pronounced in the outer levels, where the highest Si concentration were detected by the EDS analysis. The penetration depth of the needle at one strike, namely 2.5 mm, was reduced of approximately 30% compared to the untreated stone, where it was 4 mm. At 15 strikes the unconsolidated stone layers were likely investigated, leading to the needle penetration at the same depth in treated and untreated samples.

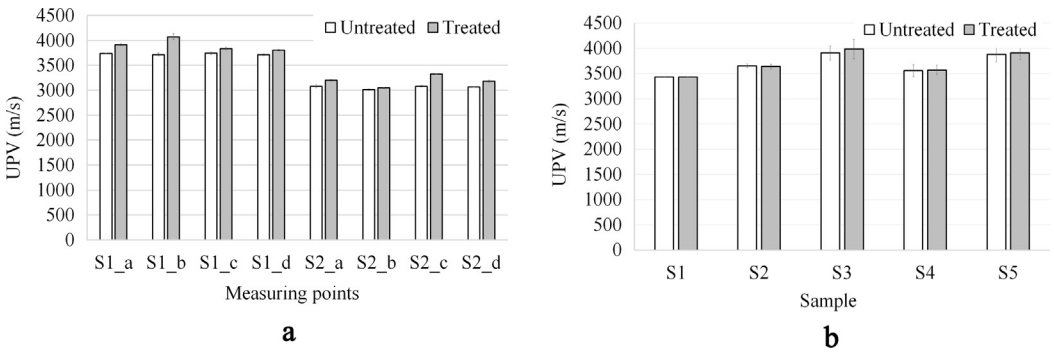

Fig. 4. a) UPVs measured on thin10 × 10 × 2 cm samples (S1 and S2) before and after the treatment at four (a, b, c, d) measuring points; b) Mean UPVs measured on five treated and untreated 5 × 5 × 5 cm stone samples.

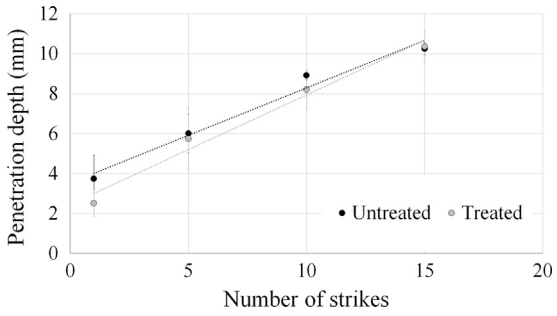

Fig. 6. Results of the penetration test obtained on the treated and untreated surface of the stone.

4.2. Compatibility

4.2.1. Colour change

The compatibility of conservation treatments, including both protective and consolidating ones, is the attitude of not altering significantly the aesthetical, physical and microstructural properties of the original stone [13]. Preservation of the colour properties of the stone surface is one of the main requirements to fulfil. In this regard, not significant variations affected the colour properties of the stone surface due to the nanosilica based treatment.

Colorimetric measurements before and after the treatment (Table 2) showed a slight decrease of L* ($\Delta L^* = 1.44$) and b* ($\Delta b^* = 1.54$). The variation of the a* parameter was almost negligible ($\Delta a^* = 0.08$). The overall colour change (ΔE^*) was 2.26, which is below the threshold value accepted in the stone conservation field and slightly higher than the colour changes visible to naked eyes [13].

4.2.2. Porosity and porosimetric features

The effect of the nanoparticle fillers on the stone microstructure, in the first 5 mm from the treated surface, consisted of a slight reduction of the integral open porosity, passing from 31% to 28% after the treatment. In addition, a shift of the pore sizes towards smaller radii was observed (Table 3). The porosimetric distribution of the stone before the treatment was mostly in the range between 0.5 μm and 4 μm (87%), with a maximum peak of 53% between 1 and 2 μm. Pores with radii under 0.5 μm were about 11%, while the coarser pore fraction, namely, with radii over 10 μm, was less than 2%. After the treatment, the most significant changes affected the pore radius dimensions between 4 and 0.5 μm. A reduction from 15% to 10% of the pores with radii between 4 and 2 μm was recorded, while those between 2 and 0.5 μm increased from 72% to 78%. Very small changes in the range of the smallest pores was detected, with a decrease of approximately 1% in the pore sizes between 0.5 and 0.1 μm and an increase at the same entity in those between 0.1 and 0.001 μm. According to [21], the porosimetric variations are likely due to the nanoparticles entering the stone porous structure, which produce some occlusions of the small voids and a partial filling of the bigger ones, causing the reduction of the radii. In principle, a moderate porosity decrease may be a not unwanted effect, since it might lead to a lower stone susceptibility to weathering due to a reduced penetration of decay agents [43]. On the contrary, variations in pore size distribution deserve attention, as they may be detrimental to the durability of the treated stone [44].

4.2.3. Hydric behaviour

As regard the behaviour with water, the application of the treatment did not change the wettability of the stone surface. The contact angle measurements failed on the untreated stone, as water absorption was very high and rapid and no drop formed on its surface, and this behaviour was confirmed on the treated samples.

Porosity and especially the pore space geometry play a great role on the migration of fluids and vapour in the stone material [45]. The small reduction of the porosity and the variation of the porosimetric features in the treated samples did not have a significant effect on the absorption of water by capillarity. The curves of the capillary water uptake in Fig. 7 show negligible changes in the sample behaviour. A small decrease of the total amount of the absorbed water from 432 mg/cm^2 to 414 mg/cm^2, that is approximately 4%, was recorded (Table 4). The capillary absorption coefficient, as well, showed a slight reduction of the absorption kinetics. The former is comparable to the results obtained in the consolidation of a Tunisian bioclastic calcarenite by Zornoza-Indart and López-Arce [25], although nanosilica was applied at lower amounts in that case, while the capillary absorption coefficient follows an opposite trend. Changes in the microstructural features seem to have a higher incidence on the stone interaction with water vapour and its transfer. The measured permeability to water vapour was found to decrease (Table 4), with a reduction of 26%. Reductions measured in both capillarity absorption and permeability to the water vapour tests are notably lower than those reported for the Lecce porous limestone after the consolidation, in spite of a lower amount of the nanosilica-based sol used (45 mg/cm^2), which was applied by a pipette method, rather than by brushing [21]. It is evident how different results may be obtained from the interactions between nanoparticle dispersions and porous substrates, as a function of a complex of factors, which include the characteristics of both stones and products, the application methods and the environmental conditions of the treatments, as well.

4.3. Durability

Under salt crystallisation test, the specimens treated with the nanosilica showed visible changes since after the first ageing cycle,

Table 2
Colour parameters (L*, a* and b*) and overall colour change (ΔE*) measured on the surface of untreated and treated stone samples.

	L*		a*		b*		ΔE*	
	Mean	St. dev.	Mean	St. dev.	Mean	St. dev.	Mean	St. dev.
Untreated	93.17	0.88	0.41	0.13	5.60	0.58	–	
Treated	91.73	0.89	0.49	0.19	7.14	0.50	2.26	0.44

Table 3
Mean pore size distribution measured on untreated and treated stone samples, along with standard deviations.

Pore size (μm)	100-50	50-10	10-4	4-2	2-1	1-0.5	0.5-0.1	0.1-0.001
Untreated-Relative Volume (%)	0.27 ± 0.22	1.64 ± 0.99	0.39 ± 0.18	14.96 ± 5.38	53.42 ± 17.38	18.48 ± 1.87	8.91 ± 1.16	1.96 ± 1.57
Treated Relative Volume (%)	0.16 ± 0.03	0.88 ± 0.21	0.88 ± 0.33	9.59 ± 3.43	55.24 ± 13.36	22.46 ± 3.24	7.68 ± 0.57	3.12 ± 0.57

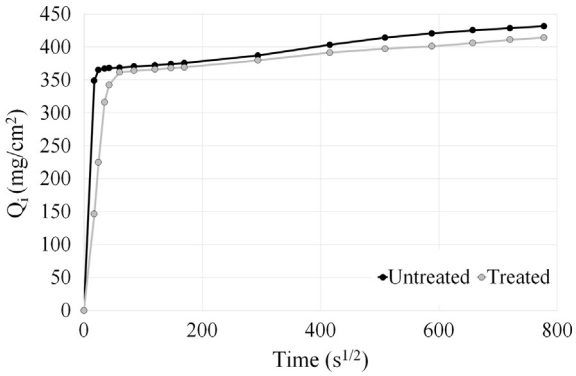

Fig. 7. Capillary water absorption curves as a function of the time over a test period of 8 days, for treated and untreated stone samples.

Table 4
Amounts of water absorbed by capillarity (Wa) at the end of a test period of 8 days, capillary absorption coefficient (A.C.) and water vapour permeability values (WVP) along with standard deviation, measured for untreated and treated stone samples.

	Wa (mg/cm^2)	A.C. (mg/cm^{2}s$^{-1/2}$)	WVP (g*m^{-2}24 h)
Untreated	432	8.30	200 ± 15
Treated	414	7.44	147 ± 18

due to the appearance of a white salt crust [46] on their overall surface. Visible cracking affected both treated and untreated samples starting from the fourth cycle. At this stage, powdering, with loss of the sample edges, started to affect the treated samples (Fig. 8a), while it was observed on the untreated ones after five cycles. From here on, contour scaling, bursting and rounding of the specimen edges (Fig. 8b) [46] were observed in both treated and untreated samples, but they had a higher incidence on the former ones. The damage progressively increased with the increasing number of cycles and most of the treated samples almost completely lost their shape, while the untreated samples preserved their faces to a larger extent (Fig. 8c).

The mean weight loss measured for treated and untreated samples after each cycle is shown in Fig. 9a. The weight variation curves typically identify three phases. They consist of an initial weight increase due to salt accumulation into the pores, followed by a weight decrease owing to competing salt accumulation and material loss. The weight decrease progressively evolves and become more pronounced because material loss becomes predominant over the salt accumulation. The weight increase due to salt accumulation into the stone microstructure was observed up to four cycles in the untreated samples and up to three cycles in the untreated ones. In both them, it was negligible (approximately between 1% and 2%). It can be supposed that during this stage the salt accumulation was offset by a slight material loss. Samples

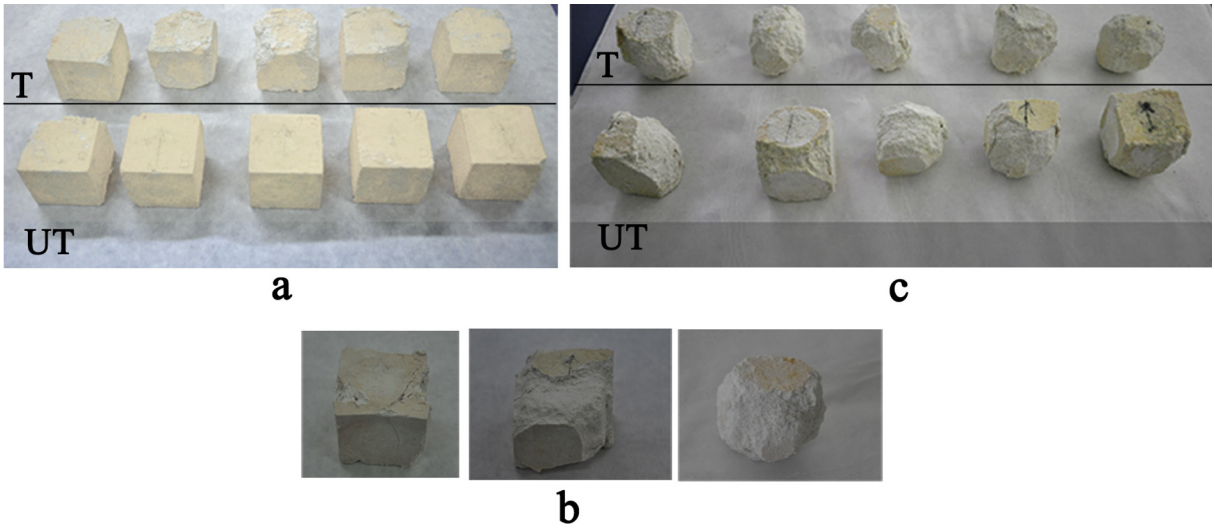

Fig. 8. Treated (T) and untreated specimens (UT) after 4 cycles (a) and 10 cycles (c) of salt crystallisation test. Detail of the fissuring, loss of sample edges and rounded shapes observed in both treated and untreated samples (b).

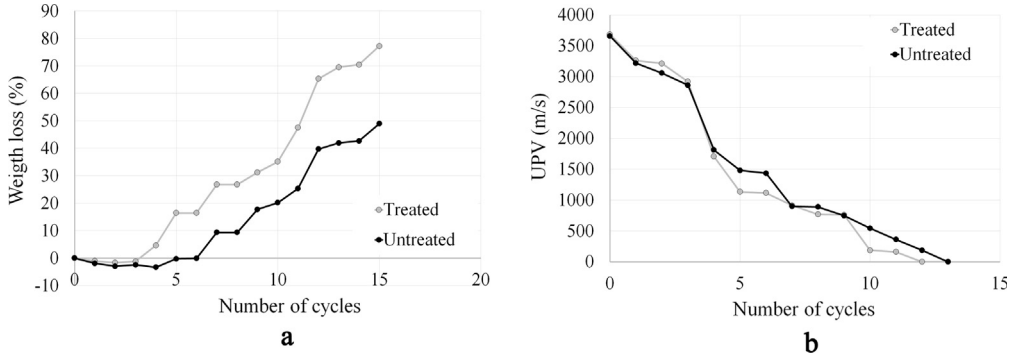

Fig. 9. Weight loss (a) and UPVs (b) measured for treated and untreated specimens at the end of each salt crystallisation cycle.

consolidated with nanosilica started to significantly lose their weight at the fourth cycle, according to the damage visually observed at this stage, and they maintained this behaviour over the whole ageing cycles. At the end of the test, the recorded weight loss was 77%. The untreated samples exhibited a higher resistance to the salt crystallisation test. Their weight loss became significant after seven cycles and the final value was 49%.

UPV technique is effective in investigating stone damage in a non-destructive way, before it become evident, as it is able to detect fissuring and microcracks through velocity variations [47–49]. A decrease of the UPVs was recorded during the salt crystallization test. The mean values of the propagation velocities obtained for treated and untreated samples at the end of each ageing cycle is reported in Fig. 9b. From the first to the third cycle, a gradual reduction of UPV, at comparable entities, was registered in both them. This reduction may be attributed to micro-cracks and micro-fractures, not visible to naked eyes, due to the salt crystallization within the pore network of the stone [50,51]. A strong reduction of the wave propagation occurred after four cycles, irrespective of the presence of the treatment, recording a similar damage in the bulk of treated and untreated stone, but corresponding to a higher weight loss in the former ones. This drop was due to the presence of visible macro-cracks, stopping the transit of the elastic waves. At this stage, a zero value of UPV was registered in two treated specimens and two untreated ones. Starting from this cycle, UPV values were slightly lower for the treated samples compared to the untreated ones, thus evidencing a higher damage due to salt growth for the stone in the presence of nanosilica, according to the weight loss results.

Fig. 10 shows a correlation between the weight loss at the end of the ageing cycles and UPVs measured in the untreated samples before the salt ageing test that is the higher the values of UPV, the lower the entity of the weight loss. Also for the treated sample group the values of UPVs were inversely proportional to the weight loss amounts at the end of the test. A relationship between ultrasonic wave velocities and resistance to the salt crystallisation effects of natural stones is reported in literature [52,53]. This is because UPV depends on several stone properties such as mechanical strength, elasticity, density and porosity, which are also relevant to the stone resistance to the salt damage. Nonetheless, if we compare the two sample groups, the treated samples show a higher weight loss than the untreated samples, although they have a UPV equal or larger compared to that of the latter ones. This occurs in spite of the fact that a higher ultrasonic wave velocity might suggest a higher degree of cohesion of the treated samples, according to the increased surface hardness. This behaviour may be due to the fact that the consolidant product into the stone pore structure also modifies important features beyond the cohesion

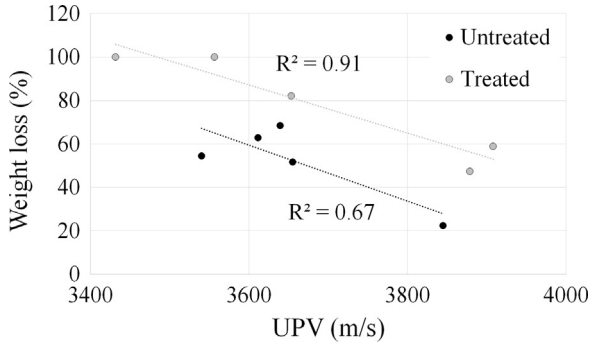

Fig. 10. Correlation between the weight loss at the end of the salt crystallisation test and UPVs registered before weathering on each treated and untreated specimen.

properties that may be detected by UPV and surface hardness tests, as e.g. the size of the pores, which is another basic parameter affecting the stone durability performances. Actually, complex factors inherent to the petrophysical and mechanical characteristics of the stone, influence the incidence of the damage due to salt crystallization, as they are relevant to the transport of the solution within the porous network, as well as to the stone resistance to the crystallization pressures [54,55]. In particular, the porous network characteristics and their modification, along with the petrographic features may account for the high susceptibility to salt damage observed for the untreated stone and further increased in the presence of the applied treatment. High stone porosity – at similar entities before and after the treatment – plays a significant role, as it involves a high mass exposure to the penetration of the saline solution [56]. In addition, pore sizes may be critical as the maximum crystallisation pressures and the consequent disruptive effects of the salt growth can be developed within the small voids [53,57]. A high susceptibility to salt damage of the Carovigno stone relates to the porous microstructure, with prevailing small pores, namely in the range between 2 and 0.5 mm radii, and also results from a weak fabric due to low cement/matrix ratio and poor textural characteristics of the cement [29]. The higher damage in the presence of the nanosilica based treatment mainly comes from the more pronounced powdering and consequent higher weight loss from the most external stone layers, namely those involved in the treatment. This behaviour may be correlated to the modification of the porosimetric structure due to the nanoparticle fillers, whose most significant effect was found in the reduction of the pore presence between 4 and 2 μm radii and a corresponding increase of those with radii from 2 μm up to 0.5 μm, where a higher stress caused by the salt growth may be expected. Also finer pores under 0.1 μm in radius were found to increase, but to a negligible extent. Moreover, a low contribution to the decay is expected by these pores, as they are lesser accessible to water and saline solutions [58]. Zornoza-Indart et al. [26] also report a salt damage on a calcarenitic substrate in the presence of nanosilica due to the reduction of the porosity and the generation of micropores, whose entity was dependent on the dry or humid consolidation environments.

The pore size decrease and its detrimental effect to the durability of the treated stone may be due to an excess of nanosilica in the outer stone layers coming from the inhomogeneous distribution within the stone substrate. As reported by Licchelli et al. [24], the weight loss from Lecce stone under salt crystallization test was less pronounced when a more homogeneous distribution of nanosilica into the substrate was obtained by brushing compared to the application by capillarity.

It is not evident that a barrier effect against the migration of the saline solution toward the surface was created by the treatment. The capillary water absorption had not significant variations, while the permeability reduction was not pronounced and remained in the acceptable ranges of stone conservation treatments [59,60]. Moreover, no peculiar decay morphologies and relevant to such an effect, such as detachments of the most external stone layers, namely those involved in the treatment, were observed in the treated samples compared to the untreated ones.

5. Conclusions

An experimental campaign under laboratory conditions was carried out to assess the effects of a nanosilica-based consolidant applied on a soft and porous limestone. The stone performances were investigated by several analyses and tests, taking into account basic requirements of effectiveness and compatibility of the treatment with the characteristics and properties of the untreated stone, as well as durability of the treated stone.

The effectiveness in terms of the ability of the consolidant to penetrate into the substrate and to increase the mechanical performance of the treated surfaces was verified. Under suitable treatment procedure, tuned on the specific substrate characteristics, no accumulation of nanosilica was found on the stone surface. A surface hardness increase was found by a destructive abrasion test. Accordingly, a low-intrusion penetration test recorded a higher resistance of the consolidated stone up to the nanosilica penetration depth of 8 mm from the surface that was as measured by EDS, and non-destructive ultrasonic wave propagation measurements detected velocity increases in the treated samples, although at low entities, denoting an improved stone cohesion.

The treatment was compatible with the colour properties of the stone. It did not have significant effects on the wettability and water capillary absorption properties, while a water vapour permeability decrease was found.

While treated and untreated stones showed similar morphologies of decay under salt crystallisation test, and UPVs detected a similar damage in the bulk of both them, a higher material loss by powdering from the treated surface denoted a larger decay in the presence of the consolidation treatment. A reduction of the pore radii measured by porosimetric analyses due to silica nanoparticle fillers within the stone porous structure may account for an increased stone susceptibility to the salt damage. This effect could be due to the inhomogeneous distribution observed within the stone, leading to an excess of the applied product in the outer stone levels. This is an open issue to be addressed by a suitable optimization of the colloidal dispersion for improving the xerogel distribution within the stone structure, as well as of the applied amounts, under a correct balancing with the consolidation efficacy.

Declaration of Competing Interest

None.

Acknowledgements

This research was developed in the frame of the the A.I.Te.C.H. (Applied Innovation Technologies for Diagnosis and Conservation of Built Heritage) Network of research laboratories, supported by the 2007-2013 FESR-FSE Puglia Funds.

References

[1] M. Steiger, A.E. Charola, K. Sterflinger, Weathering and Deterioration, Springer, Berlin Heidelberg, Berlin, Heidelberg, 2011. doi: 10.1007/978-3-642-14475-2.
[2] G. Wheeler, Alkoxysilanes and the consolidation of stone, J. Am. Inst. Conserv. 46 (2005) 189–191, https://doi.org/10.1007/s13398-014-0173-7.2.
[3] G. Scherer, G. Wheeler, Silicate consolidants for stone, Key Eng. Mater. 391 (2009) 1–25.
[4] M.J. Mosquera, D.M. de los Santos, L. Valdez-Castro, L. Esquivias, New route for producing crack-free xerogels: obtaining uniform pore size, J. Non-Cryst. Solids 354 (2-9) (2008) 645–650, https://doi.org/10.1016/j.jnoncrysol.2007.07.095.
[5] B. Sena da Fonseca, A.P. Ferreira Pinto, S. Piçarra, M.F. Montemor, The potential action of single functionalization treatments and combined treatments for the consolidation of carbonate stones, Constr. Build. Mater. 163 (2018) 586–599, https://doi.org/10.1016/j.conbuildmat.2017.12.126.
[6] Y.K. Sang, C.S. Man, Y.K. Un, J.K. Hyung, Conservation study of stones by using acrylic monomer, Polymer 32 (2008) 213–218.
[7] C. Selwitz, Epoxy resins in stone consolidation, Getty Conservation Institute, Los Angeles, 1992. http://cataleg.ub.edu/record=b1460995~S1*cat.
[8] E. Tesser, L. Lazzarini, S. Bracci, Investigation on the chemical structure and ageing transformations of the cycloaliphatic epoxy resin EP2101 used as stone consolidant, J. Cult. Herit. 31 (2018) 72–82, https://doi.org/10.1016/j.culher.2017.11.002.
[9] M. Favaro, R. Mendichi, F. Ossola, U. Russo, S. Simon, P. Tomasin, P.A. Vigato, Evaluation of polymers for conservation treatments of outdoor exposed stone monuments. Part I: Photo-oxidative weathering, Polym. Degrad. Stab. 91 (2006) 3083–3096, https://doi.org/10.1016/j.polymdegradstab.2006.08.012.
[10] E. Hansen, E. Doehne, J. Fidler, J. Larson, B. Martin, M. Matteini, C. Rodriguez-Navarro, E.S. Pardo, C. Price, A. de Tagle, J.M. Teutonico, N. Weiss, A review of selected inorganic consolidants and protective treatments for porous calcareous materials, Stud. Conserv. 48 (2003) 13–25, https://doi.org/10.1179/sic.2003.48.Supplement-1.13.
[11] E. Sassoni, G. Graziani, E. Franzoni, An innovative phosphate-based consolidant for limestone. Part 1: effectiveness and compatibility in comparison with ethyl silicate, Constr. Build. Mater. 102 (2016) 918–930, https://doi.org/10.1016/j.conbuildmat.2015.04.026.
[12] M. Matteini, S. Rescic, F. Fratini, G. Botticelli, Ammonium phosphates as consolidating agents for carbonatic stone materials used in architecture and cultural heritage: preliminary research, Int. J. Archit. Herit. 5 (2011) 717–736, https://doi.org/10.1080/15583058.2010.495445.
[13] J. Delgado Rodrigues, A. Grossi, Indicators and ratings for the compatibility assessment of conservation actions, J. Cult. Herit. 8 (2007) 32–43, https://doi.org/10.1016/j.culher.2006.04.007.
[14] E. Doehne, C.A. Price, Stone conservation: an overview of current research, 2nd ed., Getty Conservation Institute, Los Angeles, 2010. http://discovery.ucl.ac.uk/1004045/ (accessed March 5, 2012).
[15] F. Xu, D. Li, Q. Zhang, H. Zhang, J. Xu, Effects of addition of colloidal silica particles on TEOS-based stone protection using n-octylamine as a catalyst, Prog. Org. Coat. 75 (2012) 429–434, https://doi.org/10.1016/j.porgcoat.2012.07.001.
[16] A. Verganelaki, C. Kapridaki, P. Maravelaki-Kalaitzaki, Modified Tetraethoxysilane with nanocalcium oxalate in one-pot synthesis for protection of building materials, Ind. Eng. Chem. Res. 54 (2015) 7195–7206, https://doi.org/10.1021/acs.iecr.5b00247.
[17] D. Chelazzi, R. Camerini, R. Giorgi, P. Baglioni, Nanomaterials for the Consolidation of Stone Artifacts, in: C.M. Hosseini, I. Karapanagiotis (Eds.), Adv. Mater. Conserv. Stone, Springer International Publishing, Cham, 2018, pp. 151–173. 10.1007/978-3-319-72260-3_7.
[18] P. Baglioni, R. Giorgi, Soft and hard nanomaterials for restoration and conservation of cultural heritage, Soft Matter 2 (2006) 293, https://doi.org/10.1039/b516442g.
[19] A. Zornoza-Indart, P. López-Arce, L. López-Polín, Durability of traditional and new nanoparticle based consolidating products for the treatment of archaeological stone tools: chert artifacts from Atapuerca sites (Burgos, Spain), J. Cult. Herit. 24 (2017) 9–21, https://doi.org/10.1016/j.culher.2016.10.019.
[20] A. Zornoza-Indart, P. Lopez-Arce, N. Leal, J. Simão, K. Zoghlami, Consolidation of a Tunisian bioclastic calcarenite: from conventional ethyl silicate products to nanostructured and nanoparticle based consolidants, Constr. Build. Mater. 116 (2016) 188–202, https://doi.org/10.1016/j.conbuildmat.2016.04.114.
[21] P. Maravelaki-Kalaitzaki, N. Kallithrakas-Kontos, Z. Agioutantis, S. Maurigiannakis, D. Korakaki, A comparative study of porous limestones treated with silicon-based strengthening agents, Prog. Org. Coat. 62 (2008) 49–60, https://doi.org/10.1016/j.porgcoat.2007.09.020.
[22] A. Calia, G. Baldi, M. Masieri, C. Mazzotta, The evaluation of nanosilica performance for consolidation treatment of an highly porous calcarenite, in: 12 Th Int. Congr. Deterior. Conserv. Stone, 2012. http://iscs.icomos.org/pdf-files/NewYorkConf/calietal2.pdf.
[23] L. Falchi, E. Balliana, L. Izzo, Francesca Caterina, E. Zendri Agostinetto, Distribution of nanosilica dispersions in Lecce stone, Sci. Ca' Foscari. (2013) 1–49, https://doi.org/10.7361/SciCF-441.
[24] M. Licchelli, M. Malagodi, M. Weththimuni, C. Zanchi, Nanoparticles for conservation of bio-calcarenite stone, Appl. Phys. A 114 (2014) 673–683, https://doi.org/10.1007/s00339-013-7973-z.
[25] A. Zornoza-Indart, P. Lopez-Arce, Silica nanoparticles (SiO2): influence of relative humidity in stone consolidation, J. Cult. Herit. 18 (2016) 258–270, https://doi.org/10.1016/j.culher.2015.06.002.
[26] A. Zornoza-Indart, P. Lopez-Arce, K. Zoghlami, N. Leal, J. Simão, Marine aerosol weathering of mediterranean calcarenite stone: durability of ethyl silicate, nano Ca(OH)2, nano SiO2, and nanostructured consolidating products, Stud. Conserv. (2018) 1–17, https://doi.org/10.1080/00393630.2018.1477654.
[27] G. Baldi, Nanostructured oxides: from laboratory research to industrial applications – Multifunctional behavior of nanostructured surfaces and development of new industrial products. COST MP0904 Training School, (2012).
[28] G. Baldi, Nanotechnology for cultural heritage – Nanostructured materials for consolidation and pictorial integration in cultural heritage, 2008.
[29] A. Calia, M. Sileo, L. Matera, Provenance characterization and decay of a porous calcarenite of the Puglia region ('Pietra Gentile'), Geol. Soc. London, Spec. Publ. 391 (2014) 47–70, https://doi.org/10.1144/SP391.11.
[30] R. Dunham, Classification of carbonate rocks according to depositional texture., in: Classif. Carbonate Rocks - A Symp., 1962: pp. 108–121.
[31] ASTM D2845 – 08, Standard Test Method for Laboratory Determination of Pulse Velocities and Ultrasonic Elastic Constants of Rock., 2008.
[32] UNI EN 14157:2004, Natural stone test methods. Determination of the abrasion resistance, UNI, Milan, 2004.
[33] UNI EN 15886:2010, Conservation of cultural property - Test methods - Colour measurement of surfaces, UNI, Milan, 2010.
[34] UNI EN 15802:2010, Conservation of cultural property - Test methods - Determination of static contact angle, UNI, Milan, 2010.
[35] NorMaL Rec. 21/85, Permeabilità al Vapor d'Acqua, CNR-ICR, Rome, Italy, 1985.
[36] UNI EN 15801:2010, Conservation of cultural property - Test methods - Determination of water absorption by capillarity, UNI, Milan, 2010.
[37] UNI EN 12370:2001, Natural stone test methods – Determination of resistance to salt crystallisation, UNI, Milan, 2001.

[38] A.P. Ferreira Pinto, J. Delgado Rodrigues, Stone consolidation: the role of treatment procedures, J. Cult. Herit. 9 (2008) 38–53, https://doi.org/10.1016/j.culher.2007.06.004.
[39] L. Anania, A. Badalà, G. Barone, C.M. Belfiore, C. Calabrò, M.F. La Russa, P. Mazzoleni, A. Pezzino, The stones in monumental masonry buildings of the "Val di Noto" area: New data on the relationships between petrographic characters and physical–mechanical properties, Constr. Build. Mater. 33 (2012) 122–132, https://doi.org/10.1016/J.CONBUILDMAT.2011.12.076.
[40] Á. Török, B. Vásárhelyi, The influence of fabric and water content on selected rock mechanical parameters of travertine, examples from Hungary, Eng. Geol. 115 (2010) 237–245, https://doi.org/10.1016/j.enggeo.2010.01.005.
[41] E. Vasanelli, D. Colangiuli, A. Calia, M. Sileo, M.A. Aiello, Ultrasonic pulse velocity for the evaluation of physical and mechanical properties of a highly porous building limestone, Ultrasonics 60 (2015) 33–40, https://doi.org/10.1016/j.ultras.2015.02.010.
[42] P. López-Arce, L.S. Gomez-Villalba, L. Pinho, M.E. Fernández-Valle, M.Á. de Buergo, R. Fort, Influence of porosity and relative humidity on consolidation of dolostone with calcium hydroxide nanoparticles: effectiveness assessment with non-destructive techniques, Mater. Charact. 61 (2010) 168–184, https://doi.org/10.1016/J.MATCHAR.2009.11.007.
[43] D.T. Nicholson, Pore properties as indicators of breakdown mechanisms in experimentally weathered limestones, Earth Surf. Process. Landforms 26 (2001) 819–838, https://doi.org/10.1002/esp.228.
[44] A. Calia, M. Lettieri, A. Mecchi, G. Quarta, The role of the petrophysical characteristics on the durability and conservation of some porous calcarenites from Southern Italy Sustain. Use Tradit. Geomaterials Constr. Pract., in: R. Prikryl, A. Torok, M. Gomez-Heras, K. Miskovsky, M. Theodoridou (Eds.), Geological Society, Special Publication, London, 2015. doi: 10.1144/SP416.10.
[45] R. Přikryl, Durability assessment of natural stone, Q. J. Eng. Geol. Hydrogeol. 46 (2013) 377–390, https://doi.org/10.1144/qjegh2012-052.
[46] ICOMOS and ISCS, Illustrated Glossary of Stone Deterioration Patterns, 2008.
[47] R. Fort, M. Alvarez de Buergo, E.M. Perez-Monserrat, Non-destructive testing for the assessment of granite decay in heritage structures compared to quarry stone, Int. J. Rock Mech. Min. Sci. 61 (2013) 296–305, https://doi.org/10.1016/J.IJRMMS.2012.12.048.
[48] D.G. Aggelis, Wave propagation through engineering materials; assessment and monitoring of structures through non-destructive techniques, Mater. Struct. 46 (2013) 519–532, https://doi.org/10.1617/s11527-013-0020-x.
[49] E. Vasanelli, A. Calia, V. Luprano, F. Micelli, Ultrasonic pulse velocity test for non-destructive investigations of historical masonries: an experimental study of the effect of frequency and applied load on the response of a limestone, Mater. Struct. Constr. 50 (2017), https://doi.org/10.1617/s11527-016-0892-7.
[50] G. Barone, P. Mazzoleni, G. Pappalardo, S. Raneri, Microtextural and microstructural influence on the changes of physical and mechanical proprieties related to salts crystallization weathering in natural building stones. The example of Sabucina stone (Sicily), Constr. Build. Mater. 95 (2015) 355–365, https://doi.org/10.1016/J.CONBUILDMAT.2015.07.131.
[51] E. Molina, G. Cultrone, E. Sebastián, F.J. Alonso, Evaluation of stone durability using a combination of ultrasound, mechanical and accelerated aging tests, J. Geophys. Eng. 10 (2013), https://doi.org/10.1088/1742-2132/10/3/035003 035003.
[52] D. Benavente, M.A. García del Cura, R. Fort, S. Ordóñez, Durability estimation of porous building stones from pore structure and strength, Eng. Geol. 74 (2004) 113–127, https://doi.org/10.1016/J.ENGGEO.2004.03.005.
[53] M. Angeli, D. Benavente, J.-P. Bigas, B. Menéndez, R. Hébert, C. David, Modification of the porous network by salt crystallization in experimentally weathered sedimentary stones, Mater. Struct. 41 (2008) 1091–1108, https://doi.org/10.1617/s11527-007-9308-z.
[54] D. Benavente, N. Cueto, J. Martínez-Martínez, M.A. García del Cura, J.C. Cañaveras, The influence of petrophysical properties on the salt weathering of porous building rocks, Environ. Geol. 52 (2007) 215–224, https://doi.org/10.1007/s00254-006-0475-y.
[55] C. Cardell, F. Delalieux, K. Roumpopoulos, A. Moropoulou, F. Auger, R. Van Grieken, Salt-induced decay in calcareous stone monuments and buildings in a marine environment in SW France, Constr. Build. Mater. 17 (2003) 165–179, https://doi.org/10.1016/S0950-0618(02)00104-6.
[56] C. Figueiredo, R. Folha, A. Maurício, C. Alves, L. Aires-Barros, Pore structure and durability of Portuguese limestones: a case study, Geol. Soc. London, Spec. Publ. 331 (2010) 157–169, https://doi.org/10.1144/SP331.14.
[57] R. Rossi Manaresi, A. Tucci, Pore structure and the disruptive or cementing effect of salt crystallization in various types of stone, Stud. Conserv. 36 (1991) 53–58.
[58] O. Buj, J. Gisbert, Influence of pore morphology on the durability of sedimentary building stones from Aragon (Spain) subjected to standard salt decay tests, Environ. Earth Sci. 61 (2010) 1327–1336, https://doi.org/10.1007/s12665-010-0451-4.
[59] G. Alessandrini, M. Aglietto, V. Castelvetro, F. Ciardelli, R. Peruzzi, L. Toniolo, Comparative Evaluation of Fluorinated and Unfluorinated Acrylic Copolymers as Water-Repellent Coating Materials for Stone, J. Appl. Polym. Sci. 76 (2000) 962–977.
[60] P.N. Manoudis, A. Tsakalof, I. Karapanagiotis, I. Zuburtikudis, C. Panayiotou, Fabrication of super-hydrophobic surfaces for enhanced stone protection, Surf. Coat. Technol. 203 (2009) 1322–1328, https://doi.org/10.1016/j.surfcoat.2008.10.041.